EBioMedicine 40 (2019) 290–304

Contents lists available at ScienceDirect

EBioMedicine

journal homepage: www.ebiomedicine.com

EBioMedicine
Published by THE LANCET

Research paper

PTGER3 induces ovary tumorigenesis and confers resistance to cisplatin therapy through up-regulation Ras-MAPK/Erk-ETS1-ELK1/CFTR1 axis

Cristian Rodriguez-Aguayo [a,b,1], Emine Bayraktar [a,c,1], Cristina Ivan [a,b], Burcu Aslan [a,b], Junhua Mai [d], Guangan He [a], Lingegowda S. Mangala [b,g], Dahai Jiang [b,g], Archana S. Nagaraja [g], Bulent Ozpolat [a], Arturo Chavez-Reyes [e], Mauro Ferrari [d], Rahul Mitra [b,g], Zahid H. Siddik [a], Haifa Shen [d], Xianbin Yang [h], Anil K. Sood [b,f,g], Gabriel Lopez-Berestein [a,b,f,*]

[a] Department of Experimental Therapeutics, The University of Texas MD Anderson Cancer Center, Houston, TX 77030, USA
[b] Center for RNA Interference and Non-Coding RNA, The University of Texas MD Anderson Cancer Center, Houston, TX 77030, USA
[c] Department of Medical Biology, Faculty of Medicine, University of Gaziantep, Gaziantep 27310, Turkey
[d] Department of Nanomedicine, Houston Methodist Research Institute, Houston, TX 77030, USA
[e] Centro de Investigación y Estudios Avanzados del IPN, Unidad Monterrey, Apodaca, NL, CP. 66600, Mexico
[f] Department of Cancer Biology, The University of Texas MD Anderson Cancer Center, Houston, TX 77030, USA
[g] Department of Gynecologic Oncology, The University of Texas MD Anderson Cancer Center, Houston, TX 77030, USA
[h] AM Biotechnologies LLC, 12521 Gulf Freeway, Houston, TX 77034, USA

ARTICLE INFO

Article history:
Received 28 August 2018
Received in revised form 7 November 2018
Accepted 21 November 2018
Available online 14 January 2019

Keywords:
PTGER3
Ovarian cancer
RNA interference
Chemically modified siRNA
Cisplatin resistance
ETS1
ELK1
CFTR

ABSTRACT

Background: Inflammatory mediator prostaglandin E2–prostaglandin E2 receptor EP3 (PTGER3) signaling is critical for tumor-associated angiogenesis, tumor growth, and chemoresistance. However, the mechanism underlying these effects in ovarian cancer is not known.
Methods: An association between higher tumoral expression of PTGER3 and shorter patient survival in the ovarian cancer dataset of The Cancer Genome Atlas prompted investigation of the antitumor effects of PTGER3 downmodulation. *PTGER3* mRNA and protein levels were higher in cisplatin-resistant ovarian cancer cells than in their cisplatin-sensitive counterparts.
Findings: Silencing of PTGER3 *via* siRNA in cancer cells was associated with decreased cell growth and less invasiveness, as well as cell-cycle arrest and increased apoptosis, mediated through the Ras-MAPK/Erk-ETS1-ELK1/CFTR1 axis. Furthermore, sustained PTGER3 silencing with multistage vector and liposomal 2'-F-phosphorodithioate-siRNA–mediated silencing of PTGER3 combined with cisplatin resulted in robust antitumor effects in cisplatin-resistant ovarian cancer models.
Interpretation: These findings identify PTGER3 as a potential therapeutic target in chemoresistant ovarian cancers expressing high levels of this oncogenic protein.
Fund: National Institutes of Health/National Cancer Institute, USA.

1. Introduction

Ovarian cancer (OC) is the most lethal of all gynecological cancers. Early OC manifests very few specific symptoms, and most cases are diagnosed in advanced stages. This absence of symptoms in early disease and a lack of definitive screening methods are the primary causes of late diagnosis and decreased overall survival for patients with OC [1]. The current management of advanced epithelial OC generally consists of cytoreductive surgery followed by adjuvant chemotherapy that includes a platinum-based agent combined with paclitaxel [2,3]. Although this protocol typically induces an initial favorable response, most OCs eventually develop drug resistance, resulting in progressive disease and ultimately the patient's death [4].

The substantial role of inflammation in the pathogenesis of cancer has emerged in recent years [5,6]. Menstrual pain [7], endometriosis [8,9], and pelvic inflammatory disease [10] have been identified as possible risk factors for OC, as has malignant bowel obstruction in patients with recurrent OC [11]. Inflammatory cells and mediators such as reactive oxygen and nitrogen species, cytokines, chemokines, and prostaglandins are continuously present

* Corresponding author at: Department of Experimental Therapeutics, P.O. Box 301429, The University of Texas MD Anderson Cancer Center, Houston, TX 77030, USA.
E-mail address: glopez@mdanderson.com (G. Lopez-Berestein).
[1] These authors contributed equally to this work.

https://doi.org/10.1016/j.ebiom.2018.11.045

Research in context

Evidence before this study

Ovarian cancer (OC) is the leading cause of gynecological cancer related mortality. After initial response to therapy, there is high rate of recurrence and frequently rapid emergence of drug resistance. The pathology underlying this disease is not fully understood, but an inflammatory process is one factor suggested to participate in tumorigenesis. Recent studies indicate that PGE2, the ligand for at least four membrane-bound receptors, EP1–4, can activate cell growth and proliferation pathways in various types of cancer, including OC. However, the signaling pathway predominantly affecting OC chemoresistance is not well understood.

Added value of this study

In this study, we discovered that PTGER3 promotes drug resistance through regulation of the Ras-MAPK/Erk-ETS1-ELK1 pathway in OC cells, resulting in increased cell growth and reduced apoptosis. Using a multistage vector (MSV) system and 2′F-P2-siRNA, we achieved sustained PTGER3 silencing in xenograft models of OC, which significantly reduced tumor growth. Together, the data presented show that PTGER3 has a previously unrecognized role in the dual regulation of drug resistance and signaling pathways that are critical to cellular survival and tumorigenesis.

Implications of all the available evidence

Our findings indicate that PTGER3 is an important regulator of OC drug resistance through up-regulation of the Ras-MAPK/Erk2-ETS1-ELK1 axis in cancer cells, resulting in increased migration and proliferation and decreased apoptosis. PTGER3 is an attractive target for OC therapy.

in tumor tissues, supporting the association between cancer and inflammation [5,12].

Prostaglandin E2 (PGE2), a major COX-2 metabolite abundantly present in the cancer microenvironment, is an important mediator of immune regulation, epithelial cell growth and invasion [13–15], and epithelial survival [16]. Recent studies indicate that PGE2 can activate cell growth and proliferation pathways in various types of cancer, including OC. PGE2 exerts its multiple effects through four G protein–coupled receptors designated as EP1, EP2, EP3, and EP4 (PTGERs) [17] and through downstream components of cell proliferation pathways such as MAPK/Erk [13,15]. PGE2–prostaglandin E2 receptor EP3 (PTGER3) signaling has been shown to be critical for tumor-associated angiogenesis and tumor growth [18]. Furthermore, aberrant expression of PTGER3 has been associated with the biological hallmarks of several malignancies with negative clinical outcomes [19,20]. However, the roles of PTGER3 and its downstream effectors in chemotherapeutic resistance, metastasis, and proliferation are not well understood.

In this study, we discovered that PTGER3 promotes drug resistance through regulation of the Ras-MAPK/Erk-ETS1-ELK1 pathway in OC cells, resulting in increased cell growth and reduced apoptosis. Using a multistage vector (MSV) system and 2′F-P2-siRNA, we achieved sustained PTGER3 silencing in xenograft models of OC, which significantly reduced tumor growth. Thus, PTGER3 is an attractive target for OC therapy.

2. Methods

2.1. Cell culture and reagents and siRNA transfection

Normal ovarian cell line HIO180 and OC cell lines OVCAR-3, SKOV3-ip1, HeyA8, and A2780-PAR (all cisplatin-sensitive) and OVCAR-5 (cisplatin-resistant) were obtained from ATCC. Chemotherapy-resistant cell lines SKOV3-TR, HeyA8-MDR, and A2780-CP20 were obtained from Vivas-Mejia et al. (2011)[35] and Moreno-Smith et al. (2013)[36]. Cells were maintained in RPMI 1640 or Dulbecco modified Eagle–F12 medium (Corning Cellgro) supplemented with 10%–15% heat-inactivated FBS and 0.1% gentamicin sulfate (Gemini Bioproducts). All cell lines were maintained in 5% CO_2 and 95% air at 37 °C. SKOV3-TR cells were maintained in RPMI 1640 supplemented with 10% FBS and 150 ng/mL paclitaxel. HeyA8-MDR cells were maintained in RPMI 1640 supplemented with 10% FBS and 300 ng/mL taxol. All cell lines were screened for mycoplasma by using the MycoAlert mycoplasma detection kit (Lonza). All experiments were conducted with cell cultures at 60%–80% confluence.

The PTGER3 siRNA duplex was synthesized by Sigma-Aldrich. The siRNA target sequence was as follows: 3′-CTGCAACCTGGCCACCATT-5′. Cells were transfected with PTGER3 siRNA or non-silencing control siRNA. All siRNA transfections were carried out with Hiperfect (Qiagen) according to the manufacturer's recommended protocol. All siRNA sequences used in this study are listed in Supplementary Table 3.

2.2. Survival and correlation analysis for TCGA OC samples

We downloaded mRNA expression and clinical information for the ovarian serous cystadenocarcinoma samples profiled by TCGA from FIREHOSE Broad GDAC (http://gdac.broadinstitute.org/). Analyses were carried out in an R statistical environment (version 3.0.1) (http:///www.r-project.org/). All tests were two-sided and considered statistically significant at the 0.05 level. We performed Cox regression analysis (univariate and multivariate) for associations between survival and PTGER3 as well as known clinical parameters with data available (age, stage, and grade). We saw a consistent association between PTGER3 expression and bad outcome across the different techniques to measure mRNA abundance. For data visualization, we used the log-rank test to find the point (cut-off) with the most significant (lowest p value) split in high/low groups for RNASeq data. The Kaplan-Meyer method was then used to generate survival curves for both RNASeq and Agilent data cohorts using this cut-off. The Spearman's rank-order correlation test was applied to measure the strength of the association between genes of interest.

2.3. Western blot analysis

Whole cell lysates were prepared from cultured cells by subjecting them to ice-cold lysis buffer supplemented by protease and phosphatase inhibitor cocktails (Sigma). Proteins were isolated and then quantified with Pierce BCA Protein Assay Kit (Thermo Fisher Scientific). Total protein samples (30 μg) were subjected to electrophoresis on 7.5%, 10%, and 4% to 15%–gradient sodium dodecyl sulfate polyacrylamide gels (Bio-Rad) and then each was electrophoretically transferred onto a polyvinylidene difluoride membrane (Millipore). Membranes were blocked with non-fat dry milk, washed, and probed overnight at 4 °C with primary antibody followed by horseradish peroxidase (HRP)–conjugated secondary rabbit or mouse antibody (Cell Signaling Technology). All antibodies used in this study are listed in Supplementary Table 1. Bound antibodies were visualized by using an enhanced chemiluminescent HRP antibody detection kit (Denville Scientific).

2.4. RNA isolation and real-time PCR analysis

Total RNA was isolated from cells by using TRIzol reagent (Invitrogen), and 1 μg of each total RNA was reverse-transcribed by using Superscript III One-Step Reverse Transcription-PCR System (Invitrogen) according to the manufacturer's recommended protocol. The obtained cDNA was subjected to real-time PCR using iTaq Universal SYBR Green Super mix (BioRad).

All primers used in this study are listed in Supplementary Table 3. Glyceraldehyde-3-phosphate dehydrogenase (*GAPDH*) was used as a housekeeping gene (internal control). Thirty-nine cycles of amplification were performed under the following conditions: melting at 95 °C for 3 min; annealing at 60 °C for 30 s; and melting curve at 65 °C to 95 °C in increments of 0.5 °C.

2.5. Immunofluorescence

Cells (2.0×10^4/well) were seeded into 48-well plates and subjected to transfection with PTGER3 or control siRNA. After transfection, cells were fixed in 2% paraformaldehyde, blocked in 10% FBS overnight, and then incubated with primary rabbit polyclonal anti-human PTGER3 antibody (1:500; Cayman) followed by secondary antibody goat anti-rabbit Alexa Fluor 488 (Molecular Probes). Hoechst 33342 (1:10000, Molecular Probes) was used as a nuclear counterstain. Immunofluorescent images were captured by using a Nikon eclipse TE2000-U microscope. At least 5 random images were taken for each sample.

2.6. Cell proliferation assay

Cell viability was assayed by using the Alamar blue reagent (Thermo Fisher Scientific). Briefly, A2780-CP20 and OVCAR5 cells (1.0×10^3/well) were seeded in 96-well culture plates. Cells were treated with either cisplatin, siRNA, or in combination for 72 h. After treatment, the Alamar blue solution diluted with culture medium to a final concentration of 10% was added to each well. The absorbance was recorded by a spectrophotometer (Molecular Devices).

2.7. Apoptosis and cell cycle analysis

The resistant A2780-CP20 and OVCAR5 cell lines were transfected with non-silencing negative control or PTGER3 siRNA for 72 h and stained with the FITC-Apoptosis Detection Kit (BD Pharmingen) and propidium iodide (Molecular Probes). Apoptosis was analyzed by a FACSCalibur flow cytometer and CellQuest Pro software according to manufacturer's recommended protocol. For cell cycle analysis, the cells were fixed in 75% ethanol at −20 °C overnight. The cells then were washed with cold phosphate-buffered saline (PBS), treated with 100 μg of RNase A (Qiagen), and stained with 50 μg of propidium iodide. Cell cycle profiles were analyzed by using the FACSCalibur flow cytometer.

2.8. Wound healing assay

Cell migration was measured by a wound healing assay. A2780-CP20 and OVCAR5 cells (6.0×10^4/well) were plated onto 6-well plates for 16 h before transfection with PTGER3 or control siRNA. After transfection, cells were incubated at 37 °C until they reached 100% confluence to form a monolayer. Each cell monolayer was carefully scratched by using a p200 pipet tip, and cellular debris was removed by washing with Hanks balanced salt solution (HBSS; Gibco). Images were captured at 0, 12, 24, and 36 h (depending on cell line) after scratching with use of a phase-contrast Nikon eclipse TE2000-U microscope. The rate of migration was measured by quantifying the total distance that transfected cells migrated from the edge of the scratch toward the center of the scratch. The obtained values were expressed as percentage migration. Experiments were done 3 times in duplicate.

2.9. Invasion assay

Cell invasiveness was assessed by a transwell chamber assay. Transwell chambers (Greiner Bio One) were coated with Matrigel (Corning) containing extracellular matrix proteins. A2780-CP20 or OVCAR5 cells transfected with control or PTGER3 siRNA were suspended in serum-free medium and added into the upper Matrigel-coated chambers (5.0×10^5 cells/chamber). Complete medium containing 10% FBS was added to the lower chambers as a chemoattractant. The cells were incubated at 37 °C in 5% CO_2 for 24 h. After incubation, the cells in the upper chamber were removed with cotton swabs. Cells that invaded the lower chambers were fixed and stained using the Hema3 staining set (Protocol). Cells in 5 random fields were counted by using ImageJ 1.48v software. Experiments were repeated 3 times.

2.10. Colony formation assay

Cells were plated onto 24-well plates (300 cells/well), transfected with control siRNA or PTGER3 siRNA, and incubated at 37 °C for 1–3 weeks to form colonies. At the end of the incubation, the colonies were washed once with PBS and stained with crystal violet (0.5% *w*/*v*) and photographed in a Nikon eclipse TE2000-U microscope. ImageJ 1.48v software was used to count the number of colonies per well. A colony was defined as consisting of at least 50 cells. Each experiment was performed in quadruplicate and repeated 3 times.

2.11. Tube formation assay

Tube formation assay was performed according to the following protocol. Briefly, 50 μL of Matrigel (BD) was loaded in each well of the 96-well angiogenesis plate and incubated at 37 °C for 30 min to allow Matrigel to polymerize. RF-24 cells were seeded into 6-well plate and transfected with either control or PTGER3 siRNA for 72 h. Cells (1.5×10^4) were harvested and added into the Matrigel. The plate was then incubated at 37 °C, and tube formation was observed at 0, 6, 12, and 24 h. At 24 h, the wells were imaged using a Nikon microscope.

2.12. Chromatin immunoprecipitation assay

A2780-CP20 cells were cultured in 10% FBS to ~75% confluence, and cells were cross-linked with 37% formaldehyde (final concentration was 1%) for 20 min and were incubated with glycine (0.125 M) as previously described. Cells were lysed, and chromatin was sonicated 6 times for 10 s in each, according to the protocol provided by the kit (EZ ChIP, Upstate Biotechnology; cat #17–371). Possible binding sites of ETS1 and ELK1 in the CFTR promoter were predicted with use of an online tool (http://alggen.lsi.upc.es). Six primer pair sets were designed by using basic local alignment search tool software (National Center for Biotechnology Information). Primers used for amplification of the DNA in quantitative PCR are shown in Supplementary Table 3. Anti-ELK1 antibody, anti-ETS1 antibody were used for the chromatin immunoprecipitation assays (details are provided in Supplementary Table 1). The Bio-Rad DNA Engine Dyad Thermal Cycler (Bio-Rad) was used with the following cycling conditions: 2 min at 94 °C, followed by 35 cycles of 30 s at 94 °C, 30 s at 60 °C, and 1 min at 72 °C, followed by 1 min at 72 °C.

2.13. Sulprostrone treatment

A2780-CP20 and OVCAR5 cells (6.0×10^4/well) were seeded into 6-well plates and subjected to treatment with sulprostrone (Cayman), PTGER3 agonist, in various concentrations. After 72 h, cells were observed with use of a microscope and were then harvested for Western blot analysis.

2.14. Serum stability assay

SiRNAs (1.33 μg) were incubated in 20 μL of 10% FBS in PBS at 37 °C for up to 24 h. All samples were separated in 20% polyacrylamide gels.

2.15. Preparation of siRNA nanoliposomes and assembly into MSV

siRNAs were incorporated into 1,2-dioleoyl-sn-glycero-3-phosphocholine (DOPC; Avanti Polar Lipids, Inc.) by lyophilization. Briefly, 15 μg of siRNA and DOPC were mixed in the presence of excess t-butanol at a ratio of 1:10 (*w*/w) as described previously [21]. After addition of Tween-20, the mixture was frozen in an acetone-dry ice bath and dried. Liposomes were reconstituted by adding 40 μL of water into the vial and mixing briefly and were then loaded into discoidal porous silicon-based MSV microparticles (6×10^8) as we have previously described [22].

2.16. OC xenograft mouse model studies

Female athymic nude mice were purchased from Taconic Farms. Animal studies were conducted in accordance with the guidelines set forth by the American Association for Accreditation of Laboratory Animal Care and the US Public Health Service policy on Humane Care and Use of Laboratory Animals. All mouse studies were approved and supervised by The University of Texas MD Anderson Cancer Center Institutional Animal Care and Use Committee. All animals used were 6–8 weeks old at the time of injection.

Orthotopic models of OC were developed as described previously[24]. A2780-CP20 or OVCAR5 cells were harvested by using trypsin-EDTA, neutralized with FBS-containing medium, washed, and resuspended in appropriate numbers in HBSS before injection. To assess the therapeutic activity of MSVs, DOPC-nanoliposomes bearing either control siRNA or PTGER3 siRNA were loaded by capillarity into silicon particles to assemble MSVs for delivery of PTGER3 siRNA alone and in combination with cisplatin. Nude mice bearing A2780-CP20 tumors were randomly divided into 4 groups (4 mice/group) and treated with the following: MSV-DOPC-negative control-siRNA (15 μg control siRNA); MSV-DOPC-PTGER3-siRNA (15 μg PTGER3 siRNA); MSV-DOPC-negative control-siRNA + cisplatin (15 μg control siRNA +160 μg CIS); or MSV-DOPC-PTGER3-siRNA (15 μg PTGER3 siRNA +160 μg CIS). Cisplatin was administered intraperitoneally once weekly, and MSV/siRNA was administered intravenously biweekly. Animals were killed by cervical dislocation after 6 weeks of treatment, and tumors were removed and processed for immunohistochemical (IHC) analyses. Once mice in any group became moribund or after 6 weeks they were killed and necropsied, and tumors were harvested. Tumor weight and number and location of tumor nodules were recorded. Tumor tissue was fixed in formalin for paraffin embedding, frozen in optimal cutting temperature medium (OCT) to prepare frozen slides, or snap-frozen for lysate preparation.

2.17. IHC analysis

IHC analysis for Ki-67 was performed on 4-μm formalin-fixed paraffin-embedded epithelial cancer sections. Slides were deparaffinized and dehydrated and then subjected to antigen retrieval by using 1× Diva Decloaker (BioCare Medical) under a steamer. Endogenous peroxidases were blocked with 3% hydrogen peroxide in methanol followed by washes with PBS. Nonspecific binding was blocked with 5% normal horse serum and 1% normal goat serum in PBS. Samples were incubated with primary antibody against Ki-67 (1:200, Neomarkers) overnight at 4 °C, followed by the addition of goat anti-rabbit HRP secondary antibody (Jackson Immuno Research Laboratories) diluted in blocking solution.

IHC analyses for CD-31 were performed on 8-μm sections of fresh frozen cancer specimens embedded in OCT. Slides were fixed with cold acetone and acetone:chloroform and rehydrated with PBS. Nonspecific binding was blocked with 5% normal horse serum and 1% normal goat serum in PBS. Samples were incubated with the primary antibody, rat anti-mouse CD-31 (1:200, BD Pharmingen), overnight at 4 °C. After samples were washed, they were incubated with peroxidase-conjugated goat anti-rat secondary antibody (Jackson ImmunoResearch Laboratories). The slides were incubated with 3, 3′-diaminobenzidine (Sigma-Aldrich) at room temperature, counterstained with hematoxylin for 15 s, and mounted on a slide to be analyzed with use of a bright-field microscope.

2.18. TUNEL assay

The terminal deoxinucleotidyl transferase-mediated dUTP nick-end labeling (TUNEL) assay (Promega) was performed on 4-μm sections of fresh frozen cancer specimens embedded in OCT according to the manufacturer's recommendation. The fragmented DNA of apoptotic cells was detected by fluorescence microscopy.

2.19. Tissue platinum measurement

For analysis of the total platinum level in tumor, lung, or liver tissue samples were weighed and dissolved in benzethonium hydroxide (100 uL of benzethonium hydroxide/30 mg tissue) in a 55 °C water bath overnight. After acidification with 0.3 N HCl (4 vols), the samples were analyzed by flameless atomic absorption spectrophotometry (FAAS), and the platinum levels were determined by the method of standard addition, as described previously [23].

2.20. Statistical analysis

The Student *t*-test (unpaired, two-tailed) was used to compare independent samples from 2 different groups. All statistical tests were 2-tailed and performed by GraphPad Prism 6.0. All data were presented as mean ± standard deviation (SD). $P < .05$ was considered statistically significant.

3. Results

3.1. Elevation of PTGER3 expression is associated with poor patient survival in OC and cisplatin resistance in OC cell lines

We analyzed mRNA data from the TCGA database by using RNAseq and a microarray for patients with OC. High expression of PTGER3 was significantly associated with shorter overall survival for OC patients. The Cox regression analysis of overall survival yielded for RNASeqv2 data a hazard ratio (HR) of 1.1 (95% confidence interval [CI] = 1.01, 1.16; $p = .03$); Agilent microarray data had the same HR of 1.1 (95% CI = 1.004, 1.2; $p = .04$). High expression of PTGER3 was significantly associated with shorter disease-free survival for both the microarray and RNASeqv2 data type. The Cox regression analysis of disease-free survival yielded for the RNASeqv2 data a HR of 1.1 (95% CI = 1.03, 1.18; $p = .006$) and for the Agilent microarray data a HR of 1.15 (95% CI = 1.05, 1.25; $p = .002$). The Kaplan-Meier plots are shown in Fig. 1A and B. For Affymetrix microarray data, we found that PTGER3 was statistically significant *via* univariate regression analysis (both overall and disease-free survival), but when included in the final multivariate regression model, PTGER3 was an insignificant risk factor (data not shown).

We then analyzed the expression levels of *PTGER3* mRNA (Fig. 1C) and protein (Fig. 1D) in a panel of OC cell lines. Densitometry analysis results are presented in Fig. 1E, and the association between mRNA and protein expression in Fig. 1F (R squared = 0.850). PTGER3 was expressed at higher levels in the cisplatin-resistant cell lines (OVCAR5, SKOV3-TR, and A2780-CP20) than in its cisplatin-sensitive counterparts. Because of the high levels of PTGER3 expressed in cells from

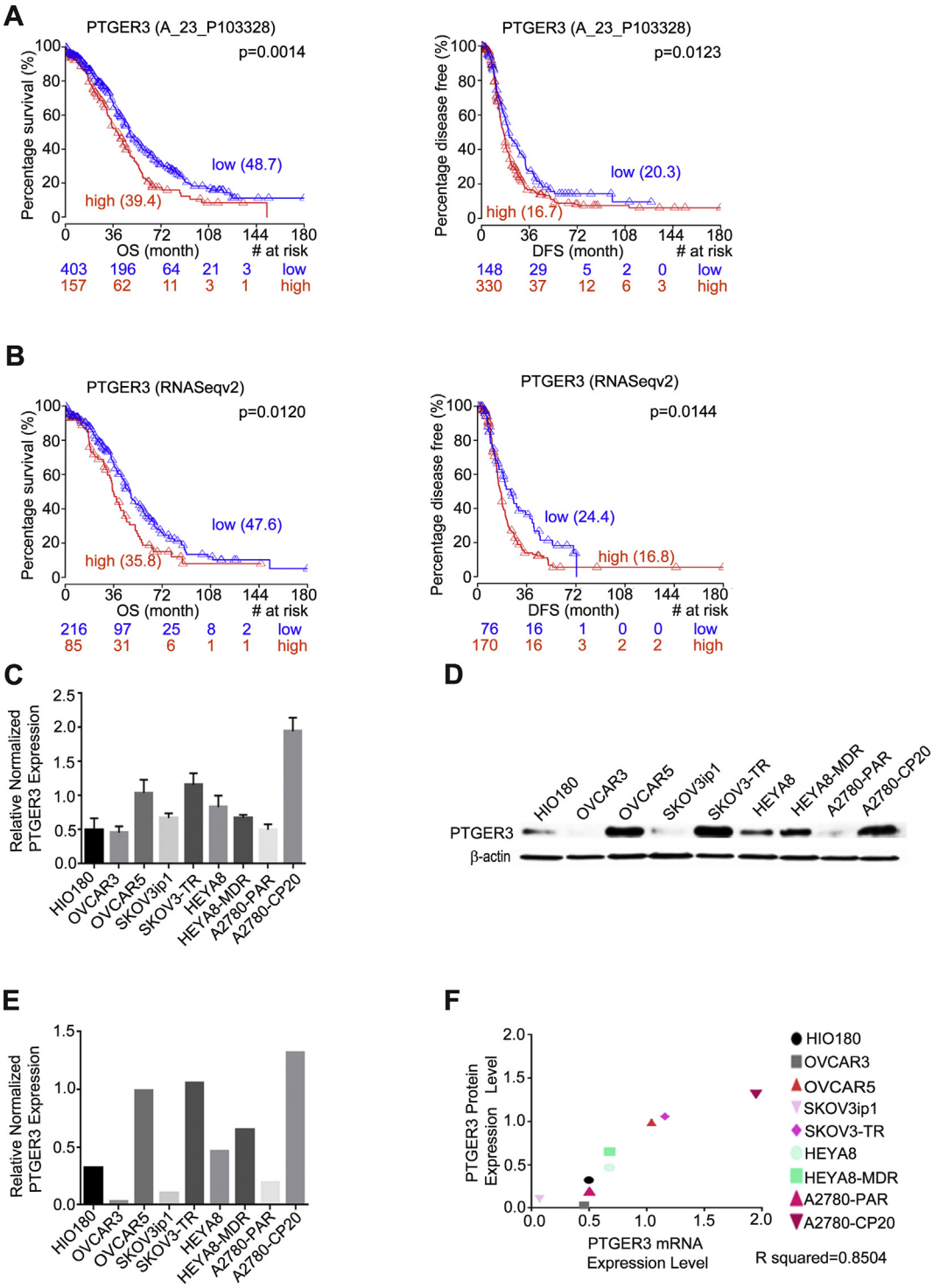

Fig. 1. PTGER3 overexpression in human tumors is associated with poor patient survival. (A, B) Statistical analysis of *PTGER3* mRNA expression and clinical data from patients with high-grade serous ovarian cancer (OC) from The Cancer Genome Atlas showed that the overall survival (OS) duration was significantly shorter for patients whose tumor expressed a higher level of PTGER3. (C, D) A panel of OC and normal ovarian cell lines was subjected to real-time PCR and Western blot analysis for PTGER3, as described in the Methods section. Beta-actin was used as a loading control. (E) Densitometric analysis of the band intensities revealed the normalized relative protein expression levels of PTGER3 in each cell line. (F) Correlation between *PTGER3* mRNA and protein levels for each cell line (R squared = 0.8504).

cisplatin-resistant cell lines A2780-CP20 and OVCAR5, these cells were used for further experiments.

4. *In vitro* suppression of PTGER3 expression reduces OC cell growth

Next, we analyzed the effect of PTGER3 silencing in two cisplatin-resistant OC models (A2780-CP20 and OVCAR5). SiRNA-mediated PTGER3 suppression was confirmed by Western blot analysis and immunofluorescence (Fig. 2A, B, and Supplementary Fig. S1A—C). Levels of *PTGER3* mRNA and protein expression were > 50% lower in the PTGER3 siRNA–transfected cells than in the control siRNA-transfected cells. Moreover, the silencing effect was specific for PTGER3, since neither PTGER1 nor PTGER2 was affected (Supplementary Fig. S2A and B).

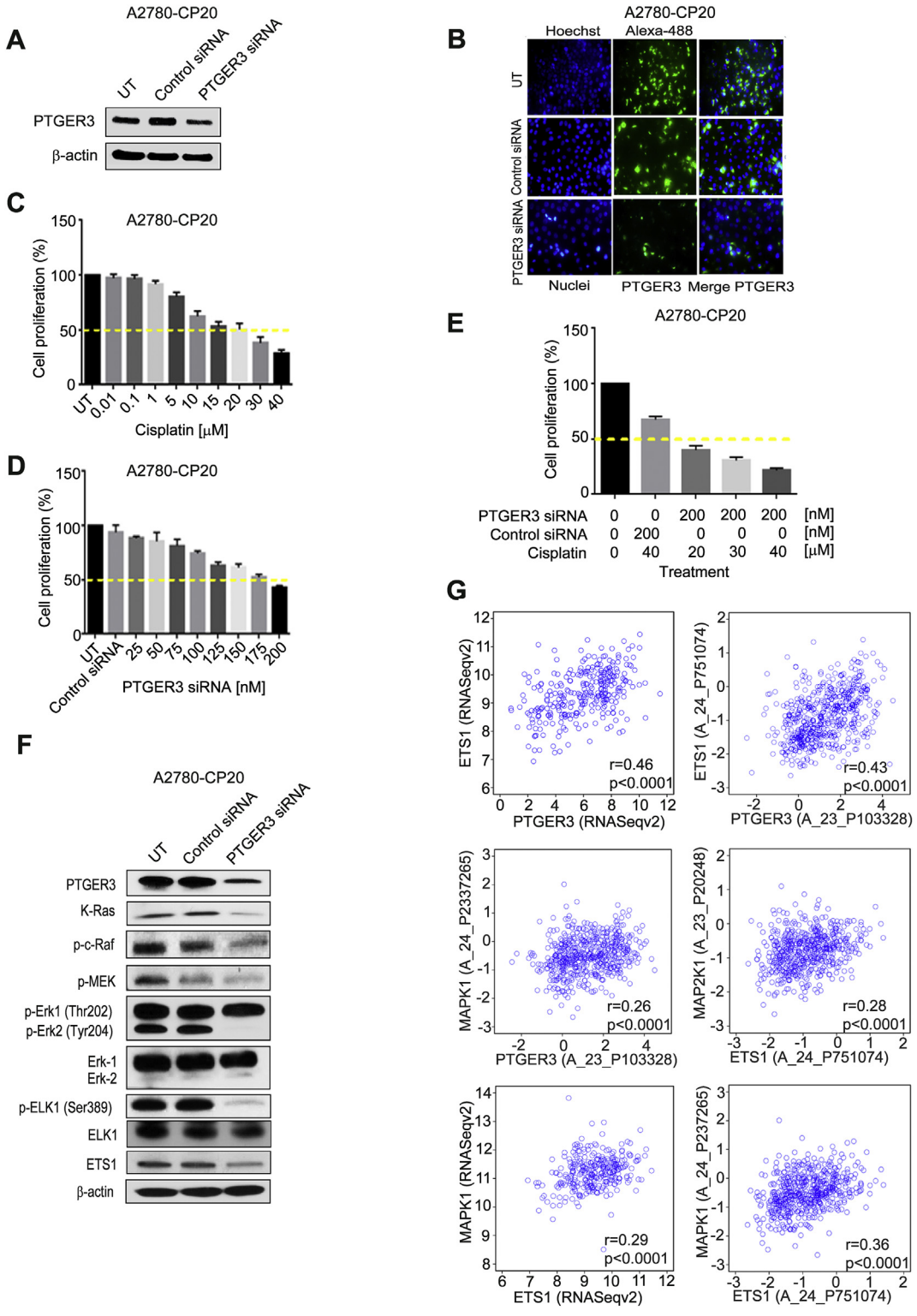

Fig. 2. siRNA-mediated silencing of PTGER3 in OC cells suppresses proliferation, increases sensitivity to cisplatin, and reduces expression of Ras-ETS1-ELK1 pathway effectors. siRNAs targeting exon 2 of the human PTGER3 sequence (NM_001126044) were used. (A, B) Total protein isolated from A2780-CP20 cells (1.6×10^4/well) transfected with PTGER3 siRNA (175 nmol/L) or control siRNA was subjected to Western blot analysis and immunofluorescence showing that the protein levels of PTGER3 were decreased. UT, untreated. (C) Dose response analysis A2780-CP20 cells (1×10^3/well). The effect of cisplatin on cell proliferation was determined after 72 h of treatment using different concentrations [20,30,40,and]. (D) A2780-CP20 cells (1×10^3/well) were transfected with control siRNA or PTGER3 siRNA at several concentrations (25, 50, 75, 100, 125, 150, 175, and 200 nM). Cell proliferation was calculated 72 h after transfection. Percentages were obtained after blank OD subtraction, taking the untreated cell values as a normalization control. Means ± SD are shown. (E) A2780-CP20 cells (1×10^3/well) were transfected with control siRNA (200 nmol/L) or PTGER3 siRNA (200 nmol/L). The next day, the medium was replaced by cisplatin in RPMI-1640 medium (CIS; 1.6 nmol/L final concentration). Cell proliferation viability was calculated 48 h after cisplatin treatment (72 h after transfection). Means ± SEM are shown. (F) A2780-CP20 cells (1.6×10^4/well) were transfected with PTGER siRNA (175 nmol/L) or control siRNA. Total protein was isolated from siRNA-transfected cells and analyzed for PTGER3 cell signaling effectors by Western blot analysis of the cell signaling of PTGER3. (G) Scatter plot graphs of the Spearman's rank-order correlation between PTGER3 and ETS1, MAPK1 and ETS1 in TCGA samples for both microarrays and RNASEqv2 data types, MAPK1 and PTGER3, MAP2K1 and ETS1 in TCGA samples for microarrays.

Next we carried out experiments to determine the responsiveness of the cisplatin-resistant A2780-CP20 and OVCAR5 cells lines to cisplatin, PTGER3 siRNA, or the combination. First, cells were treated with several concentrations of cisplatin (0.01, 0.1, 1.0, 5.0, 10.0, 15.0, 20.0, 30.0, and 40.0 μM), and growth was assessed at 72 h. As expected, the A2780-CP20 showed a cisplatin median inhibitory concentration (IC_{50}) of ~20 μM (39% inhibition; Fig. 2C). The cisplatin IC_{50} for OVCAR5 was similar, at ~20 μM (50% inhibition; Supplementary Fig. S3A). The effects of different concentrations of PTGER3 siRNA (25.0, 50.0, 75.0, 100.0, 125.0, 150.0, 175.0, and 200.0 nM) on cell growth were then evaluated; dose-dependent growth inhibition was observed after 72 h of incubation (Fig. 2D; Supplementary Fig. S3B). In A2780-CP20 cells treated with a combination of PTGER3 siRNA (200 nM) and various concentrations of cisplatin (20.0, 30.0, or 40.0 μM), PTGER3 silencing reduced the IC_{50} to <20.0 μM, unlike results seen after treatment with control siRNA (Fig. 2E). A similar effect was induced by PTGER3 silencing in OVCAR5 cells (Supplementary Fig. S3C). Control siRNA did not affect cisplatin sensitivity in either OC cell line.

It has been suggested that PGE2 can activate components of cell proliferation pathways such as MAPK/Erk [13]. To identify the potential signaling pathways in which PTGER3 is involved, we analyzed control siRNA–treated and PTGER3 siRNA–treated A2780-CP20 and OVCAR5 cells with the antibodies described in Supplementary Table 1 against several proteins and their respective phosphoproteins. Silencing PTGER3 reduced expression of the effectors of the Ras signaling pathway (Fig. 2F), K-Ras, RAF, MEK, Erk-2, and the transcriptional factors ELK1 and ETS1 (Supplementary Fig. S4A [A2780-CP20]; densitometry analysis, Supplementary Figs. S4B and S5A [OVCAR5]).

The Spearman's rank-order correlation test revealed a positive correlation between PTGER3 and ETS1 in TCGA samples for both microarrays (coefficient = 0.43) and RNASEqv2 (coefficient = 0.46) data type. We also found positive correlation between PTGER3 and MAPK1 (Erk2; coefficient = 0.26), MAP2K1 (MEK1) and ETS1 (coefficient = 0.28), MAPK1 and ETS1 (coefficient = 0.36) in TCGA samples for microarrays and MAPK1 and ETS1 (coefficient = 0.29) in TCGA samples RNASEqv2 data type. Scatter plot graphs are shown in Fig. 2G.

We previously reported that a chemical modification, consisting of phosphorodithioate (PS2), in which both non-bridging phosphate oxygen atoms are substituted with sulfur atoms, significantly improves serum stability and gene silencing over phosphoromonothioate (PS)-modified siRNAs [24]. To determine the gene-silencing activity of novel modified PTGER3 siRNAs and to gain insight into their regulation of the RNAi pathway, we first synthesized a library of modified siRNAs on solid support *via* thiophosphoramidite chemistry [25–27]. We designed PS2, 2'-OMe-PS2, and 2'-F-PS2 duplex siRNAs (Supplementary Fig. S6 and Supplementary Table 2). A2780-CP20 epithelial OC cell lines that highly express PTGER3 were transfected with modified siRNAs to test their silencing efficacy. The experiment was performed, and PTGER3 mRNA quantification was done at 48 h after transfection. 2'-OMe-PS2 and 2'-F-PS2 significantly decreased PTGER3 levels in A2780-CP20 cells compared with levels in unmodified (UM) siRNA (Fig. 3A). However, for the modification of 2`-MS2 in nucleotides 18th and 19th, and double 2'-F-PS2 modification in the nucleotides 4th and 5th in the siRNA and 10th and 11th blocked the silencing activity, these results were confirmed by Western blot analysis (Supplementary Fig. S7A, Supplementary Table 2). In particular, we found that the 2'-F-PS2 modification silenced PTGER3 to a much greater degree than did UM siRNA (four-fold enhancement). Given the potential of the 2'-F-PS2 modification in the cell line examined, we next determined the stability of the modified siRNA (2'-F-PS2) in serum. To mimic the condition in the preclinical or clinical setting, the modified siRNAs (2'-F-PS2) were incubated in a medium containing 10% fetal bovine serum (FBS). siRNA stability assays showed that half of UM siRNAs were broken down within 6 h, with near-complete degradation at 12 h. However, 2'-F-PS2 was stable for >24 h (Supplementary Fig. S8A). Next, we introduced the sequences into A2780-CP20 cells, and the PTGER3 protein levels were examined at 24, 48, 72, and 96 h after transfection. Increase in intracellular siRNA stability was confirmed with the duration of PTGER3 knockdown up to 96 h with the 2'-F-PS2 modified sequence in comparison to UM (Fig. 3B). Overall improvement in silencing and serum stability was seen for 2'-F-PS2 modified sequences compared with UM sequences (Supplementary Fig. S9A).

Having demonstrated that 2'-F-PS2-PTGER3 siRNA has superior gene-silencing activity compared with its UM counterpart, we next assessed its silencing, and in turn, we silenced the transcriptional factors ELK1 and ETS1. We then compared the therapeutic ability of an OC target gene, since acquired chemoresistance is a major contributor to patient mortality from OC, and we sought to identify targets having substantial roles in this process. Therefore, we determined the variations in expression of the MDR1 protein, as well as the multidrug resistance assosicated protein (MRP) family of drug efflux pumps. Of eight different targets, only two proteins were identified as being downregulated in A2780-CP20 OC cells after treatment of 2'-F-PS2-PTGER3, when compared with untreated or siRNA negative control. We found that MDR1 protein expression was decreased after knockdown of PTGER3, but not when we silenced either ETS1 or ELK1. Therefore, we focused on Cystic Fibrosis Transmembrane Conductance Regulator (CFTR1) (MRP7), which also showed decreased expression when PTGER3 was knocked down, as well as either ETS1 or ELK1 when we compared to untreated (UT) or the siRNA negative control (Fig. 3C).

We next investigated whether ELK1 or ETS1 transcriptionally regulates CFTR1. ELK1 or ETS1 DNA binding sites were predicted on the basis of PROMO software using version 8.3 of TRANSFAC. We identified 18 possible ETS1 binding sites and 10 ELK1 binding sites in the CFTR1 promoter by using PROMO, a virtual laboratory for the study of transcription factor binding sites in DNA sequences. The transcription start site was predicted by the ensemble approach and was compared with the CFTR1 transcript sequence and the binding locations in the CFTR1 promoter region (Fig. 3D). Six primer sets containing segments for the 18 possible ETS1 binding sites and 10 ELK1 binding sites were designed (Fig. 3D, Supplementary Table 3). DNA segments (Supplementary Fig. S10A) were amplified, cloned, sequenced, and confirmed with a standard nucleotide–nucleotide basic local alignment search tool (National Center for Biotechnology Information). To determine whether ELK1 or ETS1 binds to the promoter, we performed a chromatin immunoprecipitation (ChIP) assay in A2780-CP20 cells with ELK1 or ETS1 antibodies. Subsequent PCR results confirmed the interaction of CFTR1 promoter and four of the six predicted ELK1 or ETS1 binding sites (BS1, BS2, BS3, and BS4; Fig. 3E). A densitometric analysis of the inputs and immunoprecipitation results for each binding site revealed that BS1, BS2, and BS3 had an affinity of <50% (Fig. 3F).

These findings guided us to further analyze the link between PTGER3 and chemoresistance. Our results demonstrated that PTGER3 downregulation increased cisplatin sensitivity and compromised the proliferation of chemoresistant OC cells.

5. PTGER3 knockdown induces apoptosis and G2-M arrest

To test the effect of PTGER3 silencing on apoptosis and the cell cycle, we performed a flow cytometry analysis of A2780-CP20 and OVCAR5 OC cells for apoptosis (Fig. 4A) and analyzed the cell cycle (Fig. 4B) distribution after transfection with control siRNA or PTGER3 siRNA. Knockdown of PTGER3 significantly increased the number of cells positive for annexin V/propidium iodide staining, indicating apoptosis (A2780-CP20, 29%; OVCAR5, 45%) (Supplementary Fig. S11A). In addition, knockdown of PTGER3 induced PARP and caspase-3 cleavage and decreased levels of procaspase-9 and cytochrome C 72 h after transfection, as determined by Western blot analysis (Supplementary Fig. S12A). In line with this, G2-M cell cycle arrest was increased (A2780-CP20, 38%; OVCAR5, 42%) 48 h after PTGER3 siRNA transfection (Supplementary Fig. S11B). Western blot analysis confirmed that key proteins required for transition from the G2-M to the G1 phase were altered after

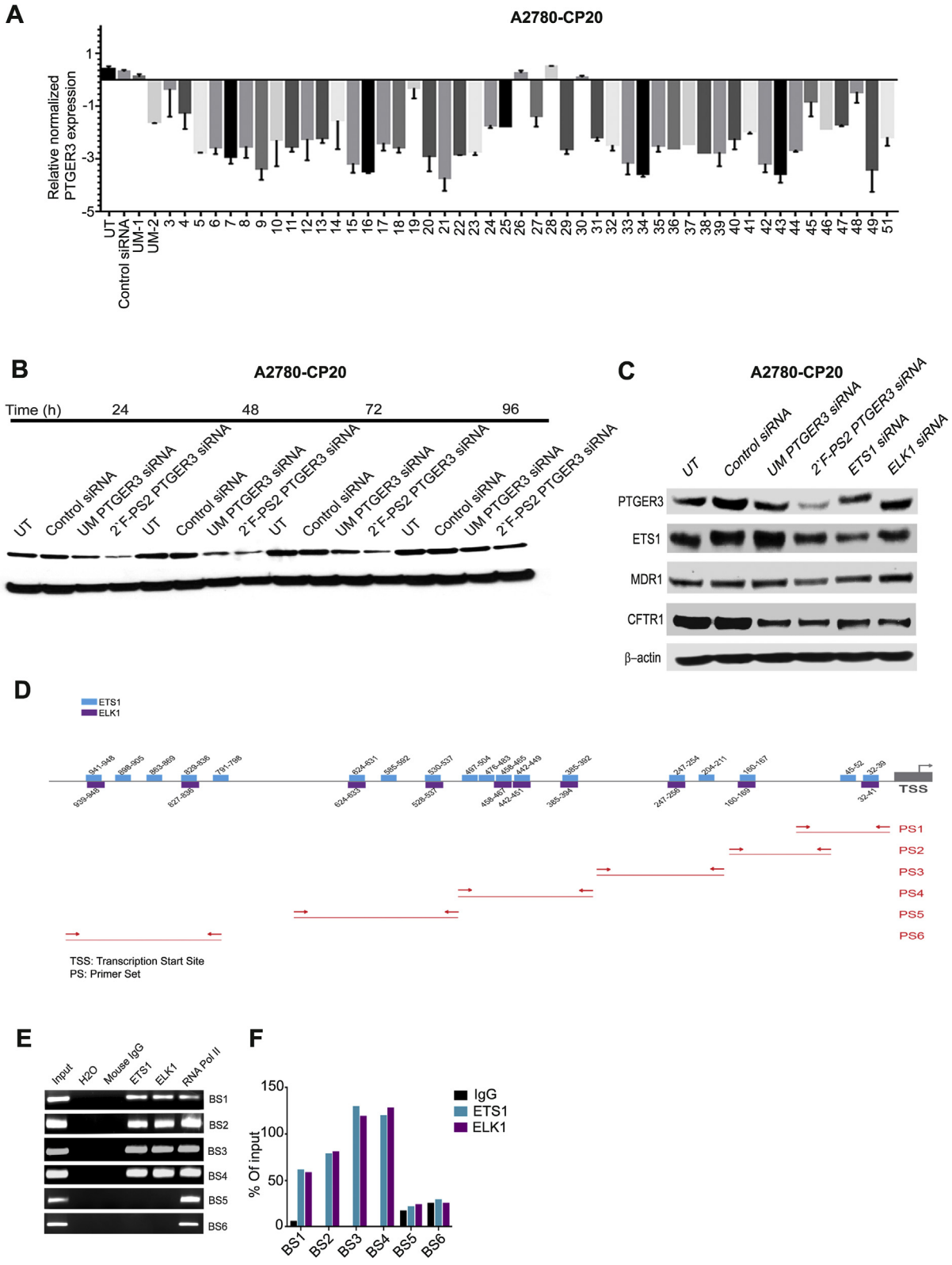

PTGER3 silencing in A2780-CP20 cells. Specifically, cyclin B1 accumulated after PTGER3 silencing and cell division cycle protein 2 homolog (Cdc2a; also known as cyclin-dependent kinase 1 [CDK]) had decreased phosphorylation on threonine 161 (T161) and tyrosine 15 (Y15), whereas proteins associated with the G1 phase of cell-cycle progression (Cdk2, Cdk4, cyclin A, cyclin D1, cyclin D3, and inhibitor p21) were unchanged compared with untreated or control siRNA–treated cells (Supplementary Fig. S13A). These results demonstrate that PTGER3 down-regulation increased apoptosis and led to cell-cycle arrest in the G2-M transition phase in chemoresistant OC cells.

5.1. PTGER3 knockdown inhibits migration, invasion, colony formation, and tube formation in OC cells in vitro

To examine the effect of PTGER3 on tumorigenic potential, we analyzed the effects of PTGER3 knockdown on migration, invasion, and colony formation in OC cells and tube formation with endothelial cells. To assess the effect of PTGER3 on migration, a wound healing assay was performed in A2780-CP20 and OVCAR5 cells after transfection with control siRNA or PTGER3 siRNA. PTGER3 knockdown cells showed significantly less migration than untreated cells or cells transfected with control siRNA after 30 h of migration time (Fig. 4C, Supplementary Figs. S14A, S15A, and S15B).

To determine the effect of PTGER3 on OC cell invasion, we transfected A2780-CP20 and OVCAR5 cells with PTGER3 siRNA (175 nmol/L) and cultured them for 72 h before harvesting and counting them for the invasion assay in Matrigel-coated transwell chambers. The percentage of invading A2780-CP20 cells was 22% ($P < .0001$) and of OVCAR5 cells was 32% ($P < .001$) (Fig. 4D, Supplementary Fig. S14B). These results indicate that PTGER3 knockdown decreased the invasiveness of both chemoresistant OC cell lines.

We also assessed the clonogenic potential of these two chemoresistant OC cell lines treated with PTGER3 siRNA (175 nmol/L). PTGER3 knockdown resulted in 4.2 times fewer A2780-CP20 and OVCAR5 colonies than did A2780-CP20 and OVCAR5 cells treated with control siRNA (Fig. 4E, Supplementary Fig. S14C).

To assess *in vitro* angiogenesis, we used the tube formation assay, as described in the Methods section. Human endothelial EC-RF24 cells were transfected with PTGER3 siRNA (175 nmol/L) or control siRNA for 72 h. After 6 h of incubation in Matrigel, the number of nodes in the endothelial cells transfected with PTGER3 siRNA was lower than that in cells treated with control siRNA or in untreated cells ($P < .001$, Fig. 4F), indicating that PTGER3 knockdown inhibits *in vitro* angiogenesis.

5.2. Treatment with a PTGER3 agonist promotes PTGER3 expression and proliferation signaling of cisplatin-resistant OC cells in vitro

To confirm the role of PTGER3 in the resistance of OC cells to cisplatin, we performed an agonistic assay in A2780-CP20 and OVCAR5 cisplatin-resistant cells. Sulprostrone, an agonist specific for PTGER3, was administered to the cells at various doses (1, 2.5, 5, or 10 μM). A2780-CP20 cell growth was dependent on Sulprostrone dose (Fig. 5A, Supplementary Fig. S16A). Western blot analysis showed that the cells stimulated with Sulprostrone expressed higher levels of PTGER3 and p-MEK1/2 proteins (Fig. 5B).

5.3. Long-lasting PTGER3 silencing restores OC sensitivity to cisplatin in vivo

On the basis of our *in vitro* findings, we examined the antitumor activity of weekly or biweekly PTGER3 silencing in two orthotopic OC cisplatin-resistant mouse models, A2780-CP20 and OVCAR5. In the former model, we tested the capacity of PTGER3 siRNA, incorporated into DOPC nanoliposomes and loaded into a MSV, to down-regulate PTGER3 expression *in vivo*; we also determined whether this PTGER3 silencing could sensitize resistant tumors to cisplatin therapy in a xenograft mouse model of OC. A week after inoculation with A2780-CP20 (cisplatin-resistant) cells, tumor-bearing mice were divided randomly into 4 treatment groups ($n = 4$ mice per group): (a) MSV-DOPC-negative control siRNA, (b) MSV-DOPC-PTGER3-siRNA, (c) MSV-DOPC-negative control siRNA + cisplatin, and (d) MSV-DOPC-PTGER3-siRNA + cisplatin. All siRNA treatments were given at 450-μg/kg of PTGER3 siRNA intravenously biweekly, and 160 μg of cisplatin was given intraperitoneally once per week. Neither control siRNA nor PTGER3 siRNA alone had a significant effect on tumor growth (Fig. 5C, left panel) or number of nodules (Fig. 5C, right panel). In contrast, treatment with MSV-DOPC-PTGER3-siRNA + cisplatin resulted in a 98% reduction in tumor growth ($P < .01$) compared with treatment with control siRNA–DOPC + cisplatin and in 98.05% less tumor growth ($P < .01$) compared with treatment with control siRNA alone (Fig. 5C).

Further examination of the biological effects of PTGER3-targeted therapy on tumor cell proliferation revealed that the mice treated with MSV-DOPC-PTGER3-siRNA as well as those treated with MSV-DOPC-PTGER3-siRNA + cisplatin had significant decreases in cell proliferation (40%, $P < .001$, and 83%, $P < .001$, respectively) compared with their corresponding controls (Ki-67; Fig. 6A upper panel, Supplementary Fig. S17A left panel). The tumors of mice treated with MSV-DOPC-PTGER3-siRNA or MSV-DOPC-PTGER3-siRNA + cisplatin showed decreased microvessel density compared with their corresponding controls (CD31; Fig. 6A middle panel). The rates of apoptosis (percentages of TUNEL-positive cells) in tumors from mice treated with MSV-DOPC-PTGER3-siRNA, control siRNA–DOPC + cisplatin, or MSV-DOPC-PTGER3-siRNA + cisplatin were considerably higher than were rates from mice treated with MSV-negative control siRNA or MSV-negative control siRNA + cisplatin. Tumors of mice treated with MSV-DOPC-PTGER3-siRNA or MSV-DOPC-PTGER3-siRNA + cisplatin had significantly higher apoptotic rates than did their corresponding controls ($P < .0001$; TUNEL; Fig. 6A, lower panel).

In the second orthotopic model (OVCAR5), the treatment groups were (i) DOPC-control siRNA, (ii) DOPC-PTGER3 siRNA, (iii) DOPC-2'-F-PS2-PTGER3 siRNA, (iv) DOPC-control siRNA plus cisplatin, (v) DOPC-PTGER3 siRNA plus cisplatin, and (vi) DOPC-2'-F-PS2-PTGER3 siRNA plus cisplatin ($n = 10$ per group). DOPC siRNA was administered intravenously every week in all treatment groups. Tumors removed from mice treated with DOPC-PTGER3 siRNA alone weighed 35% less than did those of mice treated with DOPC-control siRNA (Fig. 5D, left panel). The number of nodules was significantly reduced in mice treated with either DOPC-PTGER3 siRNA or DOPC-PTGER3 siRNA plus cisplatin (Fig. 5D, right panel). The greatest reduction was observed in the group treated with both DOPC-2'-F-PS2-PTGER3 siRNA plus cisplatin. None of the groups in either mouse model showed decreased body weight, which indicates that the treatments were not toxic (Supplementary Fig. S17B). These data indicate that inhibiting PTGER3 results in antitumor activity in mouse models of OC and that the modification of 2'-F-PS2-PTGER3 siRNA incorporated into DOPC delivery system is an efficient tool for *in vivo* gene silencing.

Given the *in vitro* and the previous *in vivo* effects of PTGER3 silencing, we performed Ki67, CD31, and TUNEL staining to examine the biological effects of silencing PTGER3 on tumor cell proliferation, angiogenesis, and apoptosis, respectively. Mice treated with either with DOPC-PTGER3 siRNA or 2'-F-PS2-PTGER3 showed significant

Fig. 3. Gene silencing of chemically modified PTGER3 siRNA and regulation of CFTR1 by ETS1-ELK1 transcriptional factors. (A) Silencing of PTGER3 with use of chemically modified siRNAs. Silencing efficiency of 2′F-PS2- and 2-OMe-modified PTGER3 siRNAs. mRNA silencing by a panel of 2′F-PS2- and 2-OMe-modified siRNAs. The PTGER3 mRNA level was assessed at 48 h after transfection. Transfection was performed at 100 nM in A2780-CP20 cells in the presence of 10% FBS. The *p*-value was obtained with a Student *t*-test; *, $p < .05$, compared with unmodified (UM) PTGER3 siRNA; bars and error bars represent mean values and the corresponding S.E.M.s ($n = 3$). UT, untreated. (B) Silencing effect of UM and 2′F-PS2 PTGER3 siRNAs on the protein level of PTGER3 in A2780-CP20 cells in a time-dependent manner (100 nM, 10% FBS containing media). (C) A2780-CP20 cells (1.6×10^4/well) were transfected with UM, 2′F-PS2 PTGER3 siRNA, ETS1, ELK1 (100 nmol/L) or control siRNA. Total protein was isolated from siRNA-transfected cells and analyzed for resistant effectors by Western blot analysis of the cell signaling of PTGER3. (D) The 18 predicted binding sites of ETS1 (blue) and the 10 predicted binding sites of ELK1 (purple) in the CFTR promoter on the basis of support vector machine scores using an online tool, available at http://alggen.lsi.upc.es. Six different primer sets were designed for the ETS1 and ELK1 predicted binding sites. (E) Chromatin immunoprecipitation (ChIP) analyses with ETS1 and ELK1 antibodies in A2780-CP20 cells. Relevant sequences were quantified by PCR with the six designed primers subsequent to ChIP assay. (F) Densitometric analysis of ChIP data. Sequence and antibody-specific controls were included. Data are presented as percentage of input.

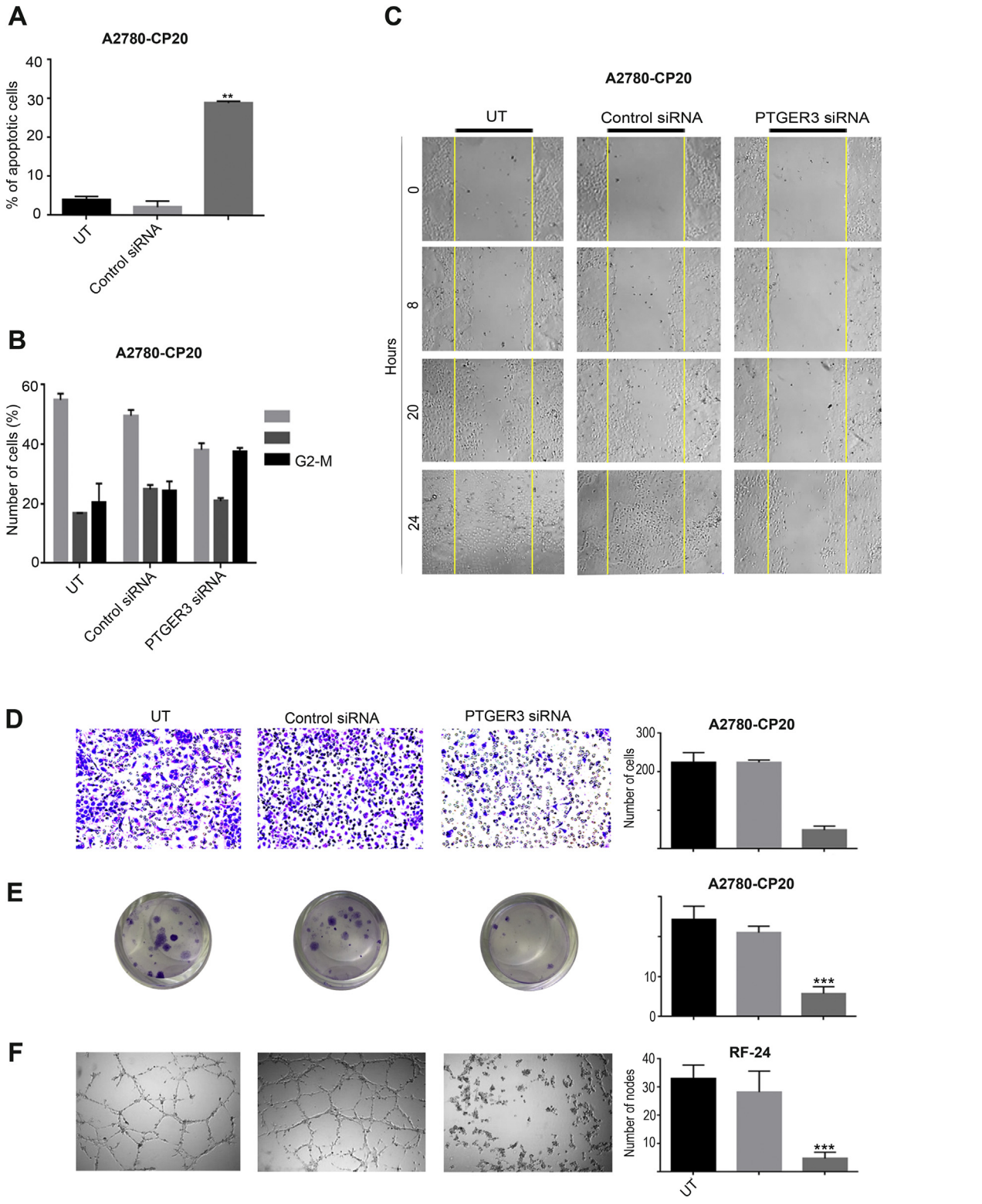

Fig. 4. PTGER3 silencing promotes apoptosis and cell-cycle arrest and inhibits migration, invasion, colony formation, and angiogenesis of ovarian cancer (OC) cells. Apoptosis and cell-cycle progression were assessed by flow cytometry after siRNA-mediated PTGER3 silencing in cisplatin-resistant OC cells. (A) A2780-CP20 cells (6×10^4/well) were transfected with PTGER3 siRNA (175 nmol/L) or control siRNA. After 72 h, apoptosis was measured with an FITC apoptosis detection kit. Means ± SD are shown for 3 independent experiments. **, $P < .01$. UT, untreated. (B) A2780-CP20 cells (6×10^4/well) were transfected with PTGER3 or control siRNA as in (A); 48 h after transfection, the cells were fixed and cell-cycle progression was determined on the basis of staining that was analyzed by Cell Quest software. Means ± SD are shown for 3 independent experiments. (C) A2780-CP20 cells (2×10^4/well) were transfected with PTGER3 siRNA (175 nmol/L) or control siRNA and subjected to a wound healing assay 24 h later. UT, untreated. (D) The invasiveness of A2780-CP20 cells was assessed by a transwell invasion assay after transfection of PTGER3 or control siRNA as in (A). UT, untreated. (E) A2780-CP20 cells (1.6×10^4/well) were seeded into 24-well plates and 24 h later were transfected with PTGER3 or control siRNA as in (A). After 14 days, cells were stained and colony formation scored with use of a light microscope. (F) Vascular endothelial EC-RF24 cells were transfected with PTGER3 or control siRNA for 72 h and then incubated in Matrigel for 6 h for the tube formation assay. The number of nodes was significantly lower in the PTGER3 knockdown cells than in untreated cells. For all assays, representative images are shown. Means ± SD are shown. ***, $P < .001$; ****, $P < .0001$.

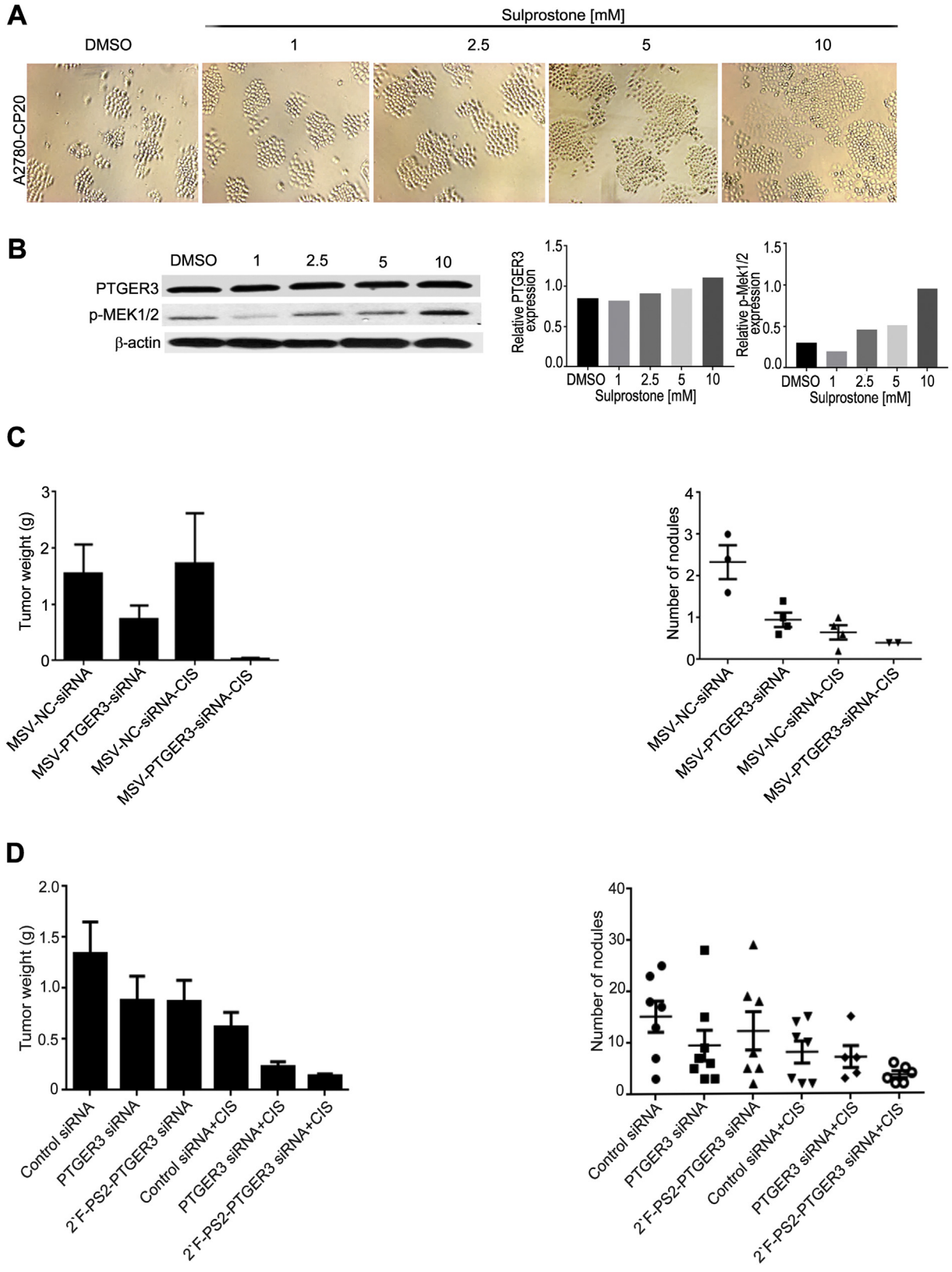

reduction in cell proliferation compared with proliferation in the control group (P*** < 0.0001; Ki-67, Fig. 6B, Fig. 17C left panel); this effect was increased when the treatment was combined with cisplatin (P*** < 0.0001).

We also examined the effects of DOPC-PTGER3 siRNA or 2'-F-PS2-PTGER3 treatment on angiogenesis. The DOPC-PTGER3 siRNA or 2'-F-PS2-PTGER3 treatments group had significantly reduced microvessel density compared with the microvessel density in the control; such effect was more prominent when the treatment was combined with cisplatin ($P \leq .0001$; Supplementary Fig. 17 middle panel). Moreover, the combination with cisplatin and the DOPC-PTGER3 siRNA or DOPC-2'-F-PS2-PTGER3 had an increase in the percentages of TUNEL-positive

cells ($P < .0001$; TUNEL, Fig. 6B lower panel, Fig. 17C right panel).These data showed that down-regulation of PTGER3 was highly associated with decreased cell proliferation, reduced microvessel density, and increased apoptosis. In further examinations, tissues were processed to evaluate the platinum tumor uptake after the treatment with DOPC-PTGER3 siRNA or DOPC-2'-F-PS2-PTGER3 in combination with cisplatin. Platinum tumor uptake was significantly increased in DOPC-PTGER3 siRNA (P^{***}, 0.45 ng platinum/mg) or DOPC-2'-F-PS2-PTGER3 (P^{*}, 0.86 ng platinum/mg) compared with DOPC-control siRNA (Fig. 6C).

These results are consistent with our *in vitro* data, indicating that long-lasting PTGER3 silencing offered by liposomal/MSV siRNA delivery or DOPC-2'-F-PS2-PTGER3 restores sensitivity to cisplatin and inhibits angiogenesis in OC cells both *in vitro* and *in vivo*.

6. Discussion

Our findings indicate that PTGER3 is an important regulator of OC drug resistance through up-regulation of the Ras-MAPK/Erk2-ETS1-ELK1 axis in cancer cells, resulting in increased migration and proliferation, and reduced tumor drug uptake and decreased apoptosis. A proposed pathway for this mechanism is shown in Fig. 7. Although PTGER3 knockdown was demonstrated to increase platinum drug accumulation in tumor xenografts, such studies were not conducted in tissue culture cells to confirm and remove the possibility that increased uptake could be an *in vivo* phenomenon. Therefore, further studies are needed to fully validate the role of PTGER3 in modulating drug accumulation. Deficiency of PTGER3 has been described as an enhancer of tumor formation [28]; however, we found that low levels of PTGER3 attenuated Ras-ETS1-ELK1 pathway–dependent tumorigenesis and drug resistance. This finding supports the key connection between inflammatory processes and cancer pathogenesis, but the mechanisms remain unclear.

In prostate cancer cells, PTGER3 limits expression of the androgen receptor, a master regulator of cell survival [19]. Sex hormones are important, either directly or indirectly, in the etiology of endometrial, breast, ovarian, and prostate malignancies. The growth and development of these organs is controlled by sex hormones, and epidemiological studies have shown that the risk of developing these cancers is associated with various hormone-related factors such as age at menarche, pregnancy, and age at menopause. There is also direct evidence that the risk of developing some of these cancers is related to the circulating serum concentration of various sex hormones [29]. Conversely, through activation of PTGER3, PGE2 sensitizes platelets to their agonists but also inhibits them through its two other receptors, PTGER2 and PTGER4. In mice, the net result of these opposed actions is that PTGER3 mediates the potentiation of platelet aggregation [30]. Increased platelet levels influence chemotherapy response in OC [31–33].

Our further demonstration revealed that the Ras-ETS1-ELK1 activation pathway was promoted by PTGER3, which was verified by silencing the expression of the receptor. The characterization of the signaling pathway showed that PTGER3 influenced a series of signaling pathways, in which most biological functions were related to the stimulation of PTGER3 by PGE2, thereby promoting proliferation and reducing apoptosis, two hallmarks of cancer development, and drug resistance. K-Ras protein is an important component of the tyrosine kinase signaling RAS/MAPK pathway. The K-Ras protein functions as a binary switch, binding GDP in its inactive state and GTP in the active, signal-emitting, state. To inactivate itself, the K-Ras protein interacts with GTPase-activating proteins (GAPs) and, when bound to GDP, it is not able to transmit signals to the cell nucleus. The hyper-activation promoted by PTGER3 or missense point mutations in the KRAS gene abolish the GTPase function and, hence, lead to a constitutively activated protein that cannot turn itself off. Inhibition of PTGER3 reduced expression of the effectors of the Ras signaling pathway. Regulating, the activation of c-Raf, MEK, Erk-2 and the transcriptional factor ELK1 and ETS1. There is growing evidence that ETS1 is involved in drug resistance. The first study linking ETS1 to resistance showed that the ETS1 level in the cisplatin-resistant OC C13* cell line was higher than that in the cisplatin-sensitive parental human 2008 OC cell line and that overexpression of ETS1 in the parental cell line resulted in cisplatin desensitization [34]. We found that ETS1 or ELK1 protein expression was decreased after knockdown of PTGER3, as well as MDR1 protein and Cystic Fibrosis Transmembrane Conductance Regulator (CFTR1) (MRP7), members of multidrug resistance assosicated protein (MRP) family of drug efflux pumps. Moreover, ETS1 or ELK1 bind to the promotor region of CFTR1, suggesting that can control its expression. However, more studies are necessary to fully validate that decrease CFTR1levels decrease platinum drug efflux. Ciglitazone enhances the cytotoxicity of cisplatin against OC cells, and the combination remarkably decreased the expression of COX-2, microsomal prostaglandin E synthase (mPGES), and PTGER3 in tumors [3]. The clinical data also showed that high PTGER3 expression is associated with poor prognosis in OC. ETS1-ELK1 also is known to promote tumorigenesis, not only in OC but also in pancreatic [35], breast [36,37], and prostate cancers [38,39].

Together, the data presented show that PTGER3 has a previously unrecognized role in the dual regulation of drug resistance and signaling pathways that are critical to cellular survival and tumorigenesis. Although this study focused on OC models, overexpression or mutations in PTGER3 in mice are also associated with endometrial cancer [40]. In conclusion, silencing of PTGER3 leads to the inactivation of ETS1-ELK1, therefore suggesting that pharmacological targeting of PTGER3 may be beneficial in individuals with a PTGER3-overexpressing tumor and can be an effective platinum-based drug sensitizer that can improve the chemotherapeutic efficacy in patients with OC.

Disclosure of potential conflicts of interest

The authors have no potential conflicts of interest to disclose. X. Yang is a full-time employee at AM Biotechnologies.

Authors' contributions

Conception and design: C. Rodriguez-Aguayo, G. Lopez-Berestein.

Development of methodology: C. Rodriguez-Aguayo, E. Bayraktar, G. Lopez-Berestein.

Acquisition of data (provided animals, acquired and treated patients, provided facilities, *etc.*): C. Rodriguez-Aguayo, E. Bayraktar, J. Mai, L.S. Mangala, B. Aslan D. Jiang, A.S. Nagaraja, B. Ozpolat, G. He, Z. H. Siddik, A. Chavez-Reyes, R. Mitra, M. Ferrari, A.K. Sood, H. Shen, X. Yang and G. Lopez-Berestein.

Fig. 5. Sulprostrone, a PTGER3 agonist, promotes expression of PTGER3 and pMEK1/2 and proliferation in ovarian cancer cells *in vitro*, and PTGER3 silencing *via* liposomal siRNA reduces tumor growth in a mouse OC orthotopic model. (A) A2780-CP20 cells (1.6×10^4/well) were treated with DMSO (vehicle control) or with PTGER3 agonist sulprostrone and observed with use of a microscope. (B) A2780-CP20 cells treated as in (A) were subjected to Western blot analysis. Compared with untreated cells, the cells stimulated with sulprostrone showed higher levels of PTGER3 and its signaling effectors p-MEK1/2. (C) Mouse xenograft ovarian tumors were established by injecting female nude mice with A2780-CP20 cells (1×10^6 cells/mouse) intraperitoneally; tumor-bearing mice were randomly allocated into treatment groups as described in the Methods section: MSV-negative control siRNA (MSV-NC-siRNA); MSV-PTGER-siRNA; MSV-NC-siRNA + cisplatin (CIS); or MSV-PTGER3-siRNA + cisplatin. Treatment began 1 wk. after tumor cell inoculation. Tumor weight and number of nodules were recorded after 4 wk. (D) Mouse xenograft ovarian tumors were established by injecting female nude mice with OVCAR5 cells (1×10^6 cells/mouse) intraperitoneally; tumor-bearing mice were randomly allocated into treatment groups as described in the Methods section: DOPC-control siRNA, (ii) DOPC-PTGER3 siRNA, (iii) DOPC-2'-F-PS2-PTGER3 siRNA, (iv) DOPC-control siRNA plus cisplatin, (v) DOPC-PTGER3 siRNA plus cisplatin, and (vi) DOPC-2'-F-PS2-PTGER3 siRNA plus cisplatin. Treatment began 1 wk. after tumor cell inoculation. (D) Tumor weight and number of nodules were recorded after 4 wk.

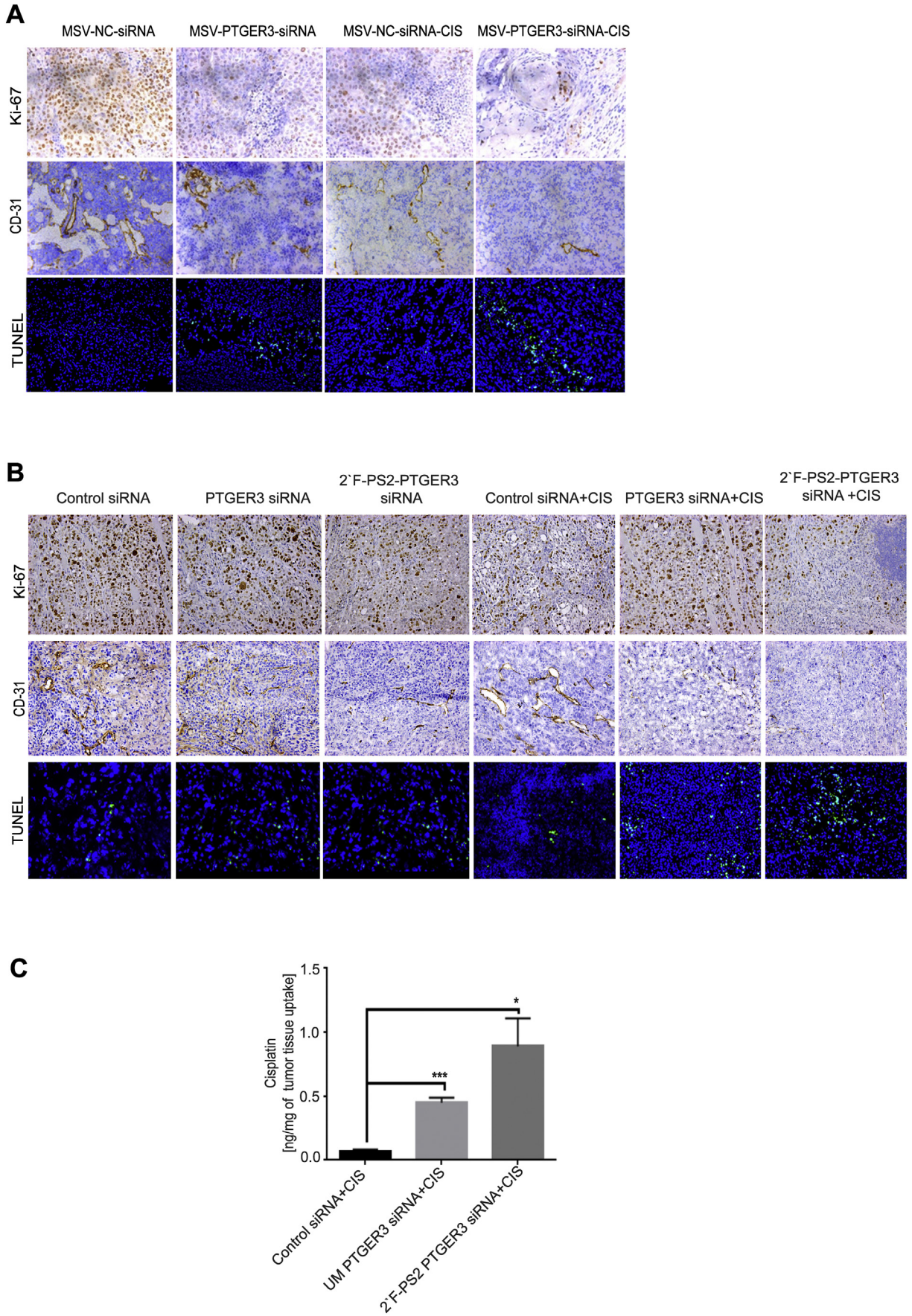

Fig. 6. Immunohistochemical analysis of Ki-67, CD-31, TUNEL and cisplatin uptake in mouse xenograft A2780-CP20 and OVCAR5 cisplatin-resistant tumors. The analysis showed that treatment with MSV-DOPC-PTGER3-siRNA or DOPC-2'-F-PS2-PTGER3 and/or combination with cisplatin reduced proliferation and angiogenesis and increased apoptosis *in vivo*. (A, B). Tumor tissue platinum uptake showed significantly greater accumulation of cisplatin in DOPC-PTGER3 siRNA and with greater uptake for DOPC-2'-F-PS2-PTGER3 in combination with cisplatin (C). Means ± SEM are shown. *, $P < .05$; **, $P < .01$; ***, $P < .001$.

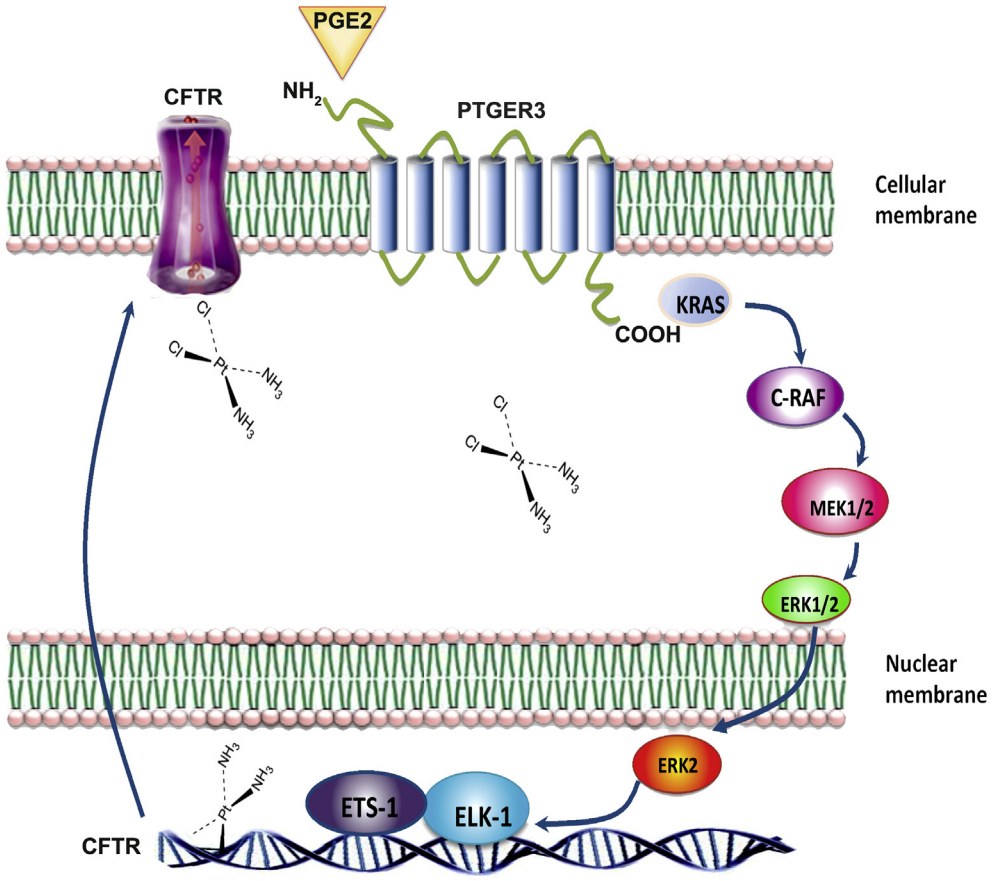

Fig. 7. Proposed model for the mechanism underlying PTGER3's role in cisplatin-resistant ovarian cancer. PGE2, a major COX-2 metabolite, can activate cell growth and proliferation through binding to PTGER3 and activating downstream components Ras-MAPK/Erk-ETS1-ELK1 in cisplatin-resistant ovarian cancer cells, resulting in increased migration, proliferation, and angiogenesis and decreased apoptosis and cisplatin uptake.

Analysis and interpretation of data (*e.g.*, statistical analysis, biostatistics, computational analysis): C. Ivan, C. Rodriguez-Aguayo, E. Bayraktar, G. He, Z. H. Siddik, A.K. Sood,

Writing, review, and/or revision of the manuscript: C. Rodriguez-Aguayo, E. Bayraktar, G. Lopez-Berestein.

Administrative, technical, or material support (*i.e.*, reporting or organizing data, constructing databases): C. Rodriguez-Aguayo, E. Bayraktar, G. Lopez-Berestein.

Study supervision: C. Rodriguez-Aguayo, G. Lopez-Berestein.

Acknowledgements

We thank Tamara K. Locke, Scientific Editor Department of Scientific Publications, Unit 1725 The University of Texas MD Anderson Cancer Center for critical reading and English editing of the manuscript.

Grant support

This work was supported in part by grants from the National Institutes of Health/National Cancer Institute (R44GM086937, P50 CA093459, U54 CA151668, P50 CA083639, P50 CA098258, R21 CA180145, UH3TR000943, RO1CA160687 and U54 CA96300), the Cancer Prevention Research Institute of Texas (RP120214), the FRANK McGraw Memorial Chair in Cancer Research, and the American Cancer Society Research Professor Award. This research was performed in the Flow Cytometry & Cellular Imaging Facility, which is supported in part by the National Institutes of Health through M. D. Anderson's Cancer Center Support Grant CA016672. The funding institutions had not any role in study design, data collection, data analysis, interpretation or writing of the report in this study.

Appendix A. Supplementary data

Supplementary data to this article can be found online at https://doi.org/10.1016/j.ebiom.2018.11.045.

References

[1] Society AC. Cancer Facts & Figures 2015. Atlanta: American Cancer Society; 2015.
[2] Gamarra-Luques CD, Goyeneche AA, Hapon MB, Telleria CM. Mifepristone prevents repopulation of ovarian cancer cells escaping cisplatin-paclitaxel therapy. BMC Cancer 2012;12:200.
[3] Yokoyama Y, Xin B, Shigeto T, Mizunuma H. Combination of ciglitazone, a peroxisome proliferator-activated receptor gamma ligand, and cisplatin enhances the inhibition of growth of human ovarian cancers. J Cancer Res Clin Oncol 2011;137(8):1219–28.
[4] Herzog TJ. Recurrent ovarian cancer: how important is it to treat to disease progression? Clin Cancer Res 2004;10(22):7439–49.
[5] Balkwill F, Mantovani A. Inflammation and cancer: back to Virchow? Lancet 2001;357(9255):539–45.
[6] Moore MM, Chua W, Charles KA, Clarke SJ. Inflammation and cancer: causes and consequences. Clin Pharmacol Ther 2010;87(4):504–8.
[7] Babic A, Cramer DW, Titus LJ, Tworoger SS, Terry KL. Menstrual pain and epithelial ovarian cancer risk. Cancer Causes Control 2014;25(12):1725–31.
[8] McKinnon B, Mueller MD, Nirgianakis K, Bersinger NA. Comparison of ovarian cancer markers in endometriosis favours HE4 over CA125. Mol Med Rep 2015;12(4):5179–84.
[9] Pavone ME, Lyttle BM. Endometriosis and ovarian cancer: links, risks, and challenges faced. Int J Womens Health 2015;7:663–72.
[10] Lin HW, Tu YY, Lin SY, Su WJ, Lin WL, Lin WZ, et al. Risk of ovarian cancer in women with pelvic inflammatory disease: a population-based study. Lancet Oncol 2011;12(9):900–4.
[11] Tran E, Spiceland C, Sandhu NP, Jatoi A. Malignant Bowel Obstruction in patients with Recurrent Ovarian Cancer. Am J Hosp Palliat Care Apr, 2016;33(3):272–5. https://doi.org/10.1177/1049909114566225 Epub 2014 Dec 31.
[12] Kundu JK, Surh YJ. Inflammation: gearing the journey to cancer. Mutat Res 2008;659(1–2):15–30.

[13] Sheng H, Shao J, Washington MK, Dubois RN. Prostaglandin E2 increases growth and motility of colorectal carcinoma cells. J Biol Chem 2001;276(21):18075–81.
[14] Pai R, Soreghan B, Szabo IL, Pavelka M, Baatar D, Tarnawski AS. Prostaglandin E2 transactivates EGF receptor: a novel mechanism for promoting colon cancer growth and gastrointestinal hypertrophy. Nat Med 2002;8(3):289–93.
[15] Krysan K, Reckamp KL, Dalwadi H, Sharma S, Rozengurt E, Dohadwala M, et al. Prostaglandin E2 activates mitogen-activated protein kinase/Erk pathway signaling and cell proliferation in non-small cell lung cancer cells in an epidermal growth factor receptor-independent manner. Cancer Res 2005;65(14):6275–81.
[16] Tsujii M, Dubois RN. Alterations in cellular adhesion and apoptosis in epithelial cells overexpressing prostaglandin endoperoxide synthase 2. Cell 1995;83(3):493–501.
[17] Dubois RN, Abramson SB, Crofford L, Gupta RA, Simon LS, Van De Putte LB, et al. Cyclooxygenase in biology and disease. FASEB J 1998;12(12):1063–73.
[18] Amano H, Ito Y, Suzuki T, Kato S, Matsui Y, Ogawa F, et al. Roles of a prostaglandin E-type receptor, EP3, in upregulation of matrix metalloproteinase-9 and vascular endothelial growth factor during enhancement of tumor metastasis. Cancer Sci 2009;100(12):2318–24.
[19] Kashiwagi E, Shiota M, Yokomizo A, Itsumi M, Inokuchi J, Uchiumi T, et al. Prostaglandin receptor EP3 mediates growth inhibitory effect of aspirin through androgen receptor and contributes to castration resistance in prostate cancer cells. Endocr Relat Cancer 2013;20(3):431–41.
[20] Ogawa F, Amano H, Eshima K, Ito Y, Matsui Y, Hosono K, et al. Prostanoid induces premetastatic niche in regional lymph nodes. J Clin Invest 2014;124(11):4882–94.
[21] Landen Jr CN, Chavez-Reyes A, Bucana C, Schmandt R, Deavers MT, Lopez-Berestein G, et al. Therapeutic EphA2 gene targeting in vivo using neutral liposomal small interfering RNA delivery. Cancer Res 2005;65(15):6910–8.
[22] Shen H, Rodriguez-Aguayo C, Xu R, Gonzalez-Villasana V, Mai J, Huang Y, et al. Enhancing chemotherapy response with sustained EphA2 silencing using multistage vector delivery. Clin Cancer Res 2013;19(7):1806–15.
[23] Kim ES, Lee JJ, He G, Chow CW, Fujimoto J, Kalhor N, et al. Tissue platinum concentration and tumor response in non-small-cell lung cancer. Journal of clinical oncology : official journal of the American Society of Clinical Oncology 2012;30(27):3345–52.
[24] Yang X, Sierant M, Janicka M, Peczek L, Martinez C, Hassell T, et al. Gene silencing activity of siRNA molecules containing phosphorodithioate substitutions. ACS Chem Biol 2012;7(7):1214–20.
[25] Xianbin Yang EM. Synthesis of nucleoside and oligonucleoside dithiophosphates. New J Chem 2010;34(5):805–19.
[26] Yang X. Thiophosphoramidites and their use in synthesizing oligonucleotide phosphorodithioate linkages. Glen Research 2008;20(1):4–6.
[27] Yang X. Solid-Phase Synthesis of Oligodeoxynucleotide Analogs Containing Phosphorodithioate Linkages. Curr Protoc Nucleic Acid Chem 2016;66 4711-414.
[28] Ma X, Aoki T, Tsuruyama T, Narumiya S. Definition of Prostaglandin E2-EP2 Signals in the Colon Tumor Microenvironment that Amplify Inflammation and Tumor Growth. Cancer Res 2015;75(14):2822–32.
[29] Key TJ, Allen NE, Verkasalo PK, Banks E. Energy balance and cancer: the role of sex hormones. Proc Nutr Soc 2001;60(1):81–9.
[30] Mawhin MA, Tilly P, Fabre JE. The receptor EP3 to PGE2: a rational target to prevent atherothrombosis without inducing bleeding. Prostaglandins Other Lipid Mediat Sep, 2015;121(Pt A):4–16. https://doi.org/10.1016/j.prostaglandins.2015.10.001 Epub 2015 Oct 14.
[31] Cho MS, Bottsford-Miller J, Vasquez HG, Stone R, Zand B, Kroll MH, et al. Platelets increase the proliferation of ovarian cancer cells. Blood 2012;120(24):4869–72.
[32] Stone RL, Nick AM, McNeish IA, Balkwill F, Han HD, Bottsford-Miller J, et al. Paraneoplastic thrombocytosis in ovarian cancer. N Engl J Med 2012;366(7):610–8.
[33] Bottsford-Miller J, Choi HJ, Dalton HJ, Stone RL, Cho MS, Haemmerle M, et al. Differential platelet levels affect response to taxane-based therapy in ovarian cancer. Clin Cancer Res 2015;21(3):602–10.
[34] Wilson LA, Yamamoto H, Singh G. Role of the transcription factor Ets-1 in cisplatin resistance. Mol Cancer Ther 2004;3(7):823–32.
[35] Khanna A, Mahalingam K, Chakrabarti D, Periyasamy G. Ets-1 expression and gemcitabine chemoresistance in pancreatic cancer cells. Cell Mol Biol Lett 2011;16(1):101–13.
[36] Kars MD, Iseri OD, Gunduz U. Drug resistant breast cancer cells overexpress ETS1 gene. Biomed Pharmacother 2010;64(7):458–62.
[37] Wei J, Zhou Y, Jiang GQ, Xiao D. Silencing of ETS1 reverses adriamycin resistance in MCF-7/ADR cells via downregulation of MDR1. Cancer Cell Int 2014;14(1):22.
[38] Kato T, Fujita Y, Nakane K, Kojima T, Nozawa Y, Deguchi T, et al. ETS1 promotes chemoresistance and invasion of paclitaxel-resistant, hormone-refractory PC3 prostate cancer cells by up-regulating MDR1 and MMP9 expression. Biochem Biophys Res Commun 2012;417(3):966–71.
[39] Smith AM, Findlay VJ, Bandurraga SG, Kistner-Griffin E, Spruill LS, Liu A, et al. ETS1 transcriptional activity is increased in advanced prostate cancer and promotes the castrate-resistant phenotype. Carcinogenesis 2012;33(3):572–80.
[40] Takahashi T, Ogawa H, Izumi K, Uehara H. The soluble EP2 receptor FuEP2/Ex2 suppresses endometrial cancer cell growth in an orthotopic xenograft model in nude mice. Cancer Lett 2011;306(1):67–75.